Parallel Evolutionary Pathways for Glutathione Transferases: Structure and Mechanism of the Mitochondrial Class Kappa Enzyme rGSTK1-1[†]

Jane E. Ladner,[‡] James F. Parsons,[§] Chris L. Rife,[§] Gary L. Gilliland,[‡] and Richard N. Armstrong*[,§]

The Center for Advanced Research in Biotechnology of the Maryland Biotechnology Institute and the National Institutes of Standards and Technology, Gudelsky Drive, Rockville, Maryland 20850, and Departments of Biochemistry and Chemistry and Center in Molecular Toxicology, Vanderbilt University School of Medicine, Nashville, Tennessee 37232-0146

Received October 9, 2003; Revised Manuscript Received November 13, 2003

ABSTRACT: The class kappa glutathione (GSH) transferase is an enzyme that resides in the mitochondrial matrix. Its relationship to members of the canonical GSH transferase superfamily has remained an enigma. The three-dimensional structure of the class kappa enzyme from rat (rGSTK1-1) in complex with GSH has been solved by single isomorphous replacement with anomalous scattering at a resolution of 2.5 Å. The structure reveals that the enzyme is more closely related to the protein disulfide bond isomerase, dsbA, from *Escherichia coli* than it is to members of the canonical superfamily. The structures of rGSTK1-1 and the canonical superfamily members indicate that the proteins folds have diverged from a common thioredoxin/glutaredoxin progenitor but did so by different mechanisms. The mitochondrial enzyme, therefore, represents a fourth protein superfamily that supports GSH transferase activity. The thioredoxin domain functions in a manner that is similar to that seen in the canonical enzymes by providing key structural elements for the recognition of GSH. The hydroxyl group of S16 is within hydrogen-bonding distance of the sulfur of bound GSH and is, in part, responsible for the ionization of the thiol in the E•GSH complex ($pK_a = 6.4 \pm 0.1$). Preequilibrium kinetic experiments indicate that the k_{on} for GSH is 1×10^5 M^{-1} s^{-1} and k_{off} for GS^- is ~8 s^{-1} and relatively slow with respect to turnover with 1-chloro-2, 4-dinitrobenzene (CDNB). As a result, the K_M^{GSH} (11 mM) is much larger than the apparent K_d^{GSH} (90 μM). The active site has a relatively open access channel that is flanked by disordered loops that may explain the relatively high turnover number (280 s^{-1} at pH 7.0) toward CDNB. The disordered loops form an extensive contiguous patch on one face of the dimeric enzyme, a fact that suggests that the protein surface may interact with a membrane or other protein partner.

GSH[1] transferases are enzymes that catalyze the addition of the thiol of GSH to electrophilic substrates. Such enzymatic activity is widespread and is associated with at least three protein superfamilies (*1*−*4*). The most extensively studied of these is the canonical GSH transferase superfamily with members that fall into various subfamilies designated as alpha, beta, delta, theta, mu, pi, sigma, phi, omega, tau, and zeta. The members of this superfamily are typically soluble dimeric proteins with subunits ($M_r \sim 25\,000$ Da) composed of a thioredoxin-like domain at the amino terminus that is fused to an all α-helical domain. The reader is directed to Board et al. (*5*) and Thom et al. (*6*) for an overview of the various structures.

Some years ago, a GSH transferase from rat mitochondrion was isolated and characterized, and its cDNA was sequenced (*7*−*9*). More recently, the gene encoding a mouse homologue has been identified and sequenced, and the enzyme has been characterized (*10*). The mitochondrial protein is a soluble dimer with a molecular mass close to that reported for the canonical superfamily members. Although the original N-terminal sequence analysis of the protein suggested a relationship with the class theta enzymes, the complete cDNA sequence was sufficiently different to warrant a separate subfamily designation, kappa (*9*). Although significant differences in sequence were noted, the similarities in size, oligomeric state, and sequence were argued to suggest that kappa was the progenitor of theta and the soluble GSH transferases and hence related by divergent evolution. In contrast, Sheehan et al. (*4*) propose that kappa represents an early divergence from an ancestral gene and not a progenitor of the canonical fold.

In the absence of a three-dimensional structure for the kappa enzyme, its relationship to the canonical superfamily has not been clear. A BLAST (*11*) analysis reveals that the closest relatives of kappa are not the soluble GSH transferases. Rather, the kappa enzyme appears to be more closely

[†] Supported by Grants R01 GM30910, P30 ES00267, T32 ES07028, and T32 GM08320 from the National Institutes of Health. Use of the Advanced Photon Source was supported by the U.S. Department of Energy, Basic Energy Sciences, Office of Science, under Contract No. W-31-109-Eng-38. Use of the BioCARS Sector 14 was supported by the National Institutes of Health, National Center for Research Resources, under Grant No. RR07707.

* To whom correspondence should be addressed. Tel: 615 343-2920. Fax: 615 343-2921. E-mail: r.armstrong@vanderbilt.edu.

[‡] The Center for Advanced Research in Biotechnology of the Maryland Biotechnology Institute and the National Institutes of Standards and Technology.

[§] Vanderbilt University School of Medicine.

[1] Abbreviations: GSH, reduced glutathione; CDNB, 1-chloro-2,4-dinitrobenzene; dsbA, protein disulfide bond isomerase; DTT, dithiothreitol; EDTA, ethylenediaminetetraacetic acid; IPTG, isopropylthiogluco-pyranoside; HEPES, 4-(2-hydroxyethyl)piperazine-1-ethanesulfonic acid; grx2, glutaredoxin-2; MOPS, 3-(N-morpholino)propanesulfonic acid; PDB, Protein Data Bank.

10.1021/bi035832z CCC: $27.50
Published on Web 12/19/2003

related to dsbA, a protein disulfide bond isomerase from *Escherichia coli* (*12*), and to the enzyme 2-hydroxychromene-2-carboxylate isomerase, a GSH-dependent enzyme in the naphthalene catabolic pathway of microorganisms (*13*). The three-dimensional structure of dsbA contains a thioredoxin-like domain and an all α-helical domain (*12*). Thus, to this extent, there is some structural similarity to the canonical GSH transferase fold. However, the domain arrangement and location are quite different in dsbA, suggesting that the two protein folds arose by alternate, perhaps parallel, evolutionary pathways.

In this report, we describe the three-dimensional structure of the class kappa enzyme from rat mitochondria (rGSTK1-1) and present a kinetic analysis of its interaction with GSH and the electrophilic substrate CDNB. The three-dimensional structure, determined at a resolution of 2.5 Å, reveals that the enzyme has the same general fold as the dsbA and consists of a thioredoxin-like domain that is interrupted with the insertion of an all α-helical domain. The structures of rGSTK1-1 and the canonical superfamily members indicate that although the proteins may have diverged from a common thioredoxin/glutaredoxin progenitor they did so by quite different mechanisms. Nevertheless, the thioredoxin domain functions in a manner that is analogous to that seen in the canonical enzymes by providing key structural elements for the recognition of GSH. Like other GSH transferases, the enzyme promotes formation of the thiolate, $E{\bullet}GS^-$, through interaction of the sulfur with the hydroxyl group of S16.

EXPERIMENTAL PROCEDURES[2]

Materials. Competent cells of *E. coli* BL21(DE3)*pLysS* were from Novagen (Madison, WI). Isopropyl-β-D-thiogalactopyranoside (IPTG) and DTT were obtained from Research Organics (Cleveland, OH). Ampicillin, chloramphenicol, sodium acetate, triethylamine, EDTA, glycerol, sucrose, MOPS, HEPES, and glutathione were purchased from Sigma (St. Louis, MO).

Cloning and Expression of rGSTK1. The class kappa gene *rGSTK1* was cloned by PCR from a rat liver cDNA library with primers designed based on the original cDNA sequence (*9*) with the inclusion NdeI and BamH1 restriction sites at the 5′- and 3′-ends of the gene, respectively. The amplified gene was cloned into the pET-20b vector and sequenced to confirm the integrity of the insert. The resulting expression vector was used to transform BL-21 (DE3) cells. The protein expression levels from this construct were very low. This problem was solved by reducing the GC content at the 5′-end of the gene by silent mutagenesis of codons 2−7 (GGG CCG GCG CCG CGC GTC→GGA CCA GCA CCA AGA GTT), 10−12 (CTG TTC TAC→TTA TTT TAT), and 14−17 (GTG CTG TCC CCC→GTA CTA TCA CCA). The new vector with optimized codons for expression in *E. coli* improved the expression levels significantly so that about 200 mg of enzyme could be purified from 10 L of BL-21 (DE3) cell culture after induction of transcription with IPTG.

Purification of rGSTK1-1. Cells containing the enzyme were harvested by centrifugation and suspended in 20 mM[3] MOPS buffer (pH 7.1) containing 100 mM NaCl, 1 mM EDTA, and 1 mM DTT. The suspended cells were lysed by sonication after which the cell debris was removed by centrifugation. The supernatant was then treated with DNAase at room temperature for 1 h. All subsequent dialysis and chromatographic steps were carried out at 4 °C. After dialysis against 4 × 4 L of 20 mM MOPS buffer (pH 7.1) containing 10 mM NaCl, 1 mM EDTA, and 1 mM DTT, the supernatant was loaded on a SP-Sepharose column (Pharmacia). The column was washed extensively with the same buffer and eluted with a 10−400 mM gradient of NaCl. Fractions containing activity toward CDNB were pooled, dialyzed against 20 mM KH_2PO_4 (pH 7.1) containing 0.5 mM EDTA and 1 mM DTT, and applied to a hydroxylapatite column equilibrated with 20 mM KH_2PO_4. The column was washed extensively with the same buffer, and the protein eluted with a linear gradient of 20−400 mM KH_2PO_4. The active fractions were pooled, concentrated, and dialyzed against 20 mM KH_2PO_4 (pH 7.1) containing 0.5 mM EDTA and 1 mM DTT for storage at −80 °C.

Crystallization. The enzyme was first dialyzed against 50 mM sodium citrate (pH 5.5). Crystals of the native enzyme were grown by the hanging drop vapor diffusion method at 4 °C. Each 15 μL drop initially consisted of 10 mg/mL protein, 0.2% β-*n*-octylglucopyranoside, 3−5 mM various ligands [GSH, glutathione sulfonate, and S-(3-iodobenzyl)-glutathione)], 0.1 M LiSO4, and 7% poly(ethylene glycol) (PEG) 3000 or PEG 6000 (pH 4.0−4.4).

Crystals of a mercury derivative of rGSTK1-1 were grown at 4°C by the method of vapor diffusion in hanging drops in the presence of CH_3HgCl using the conditions similar to those that produced crystals without mercury. The protein component of the drop was 6 mg/mL protein, 3 mM glutathione, and 0.1% β-octyl-glucopyranoside. The well solutions were 13−17% (w/v) PEG 2000, 40−80 mM lithium sulfate, and 100 mM sodium citrate, pH 4.0. Drops were made combining equal volumes of the protein solution and the well solution. The final concentration of CH_3HgCl in the drop was approximately 5 mM. As with the native enzyme, the crystals grew as thin plates, usually in clusters, and could not be brought to room temperature. Consequently, for data collection, the crystal was picked up on a loop in the cold room, dipped into a cryoprotectant solution made by combining equal volumes of well solution and 50% PEG 4000, and immediately immersed in liquid nitrogen before transferring to the X-ray goniometer.

X-ray Data Collection and Processing. Diffraction data for the mercury derivative were collected using a Rigaku Micro Max 007 rotating anode generator and a Rigaku RAXIS IV^{2+} detector (Rigaku/MSC, The Woodlands, Texas). The crystal was cooled to 100 K with a Rigaku Xtream 2000 cryocooler. Diffraction data were collected and processed with CrystalClear/d*Trek (*14*). A native data set was collected at the APS bioCARS beamline 14 BM-D and processed in DENZO (*15*). A summary of the data collection and processing statistics is given in Table 1.

[2] Certain commercial materials, instruments, and equipment are identified in this manuscript in order to specify the experimental procedure as completely as possible. In no case does such identification imply a recommendation or endorsement by the National Institute of Standards and Technology nor does it imply that the materials, instruments, or equipment identified are necessarily the best available for the purpose.

[3] The accepted SI unit of concentration, mol/L, has been represented by the symbol M in order to conform to the conventions of this journal.

Table 1: X-ray Data Collection and Processing Statistics

	Hg derivative data	native data
space group	$P2_1$	$P2_1$
cell parameters (*a*, *b*, *c*) (Å)	65.77, 111.87, 74.94	65.90, 110.79, 74.66
cell parameter (β) (deg)	101.32	101.96
wavelength (Å)	1.541	1.000
no. of measured intensities	130 960	115 187
no. of unique reflections	26 778	35 795
resolution (Å)	2.76	2.50
R_{sym} (overall/high-resolution shell)	0.100/0.250	0.072/0.166
% completeness (overall/high-resolution shell)	97.8/97.8	98.4/88.7
redundancy (overall/high-resolution shell)	2/2	4/3
mean I/σ (overall/high-resolution shell)	5.0/1.8	11.0/5.0

Structure Determination. The protein crystallized in the monoclinic space group $P2_1$. The crystal obtained in the presence of methyl mercuric chloride was isomorphous with the native crystal used for data collected at the synchrotron. Reasonable values for the Matthews constant indicated four copies of the polypeptide chain in the asymmetric unit. Initial heavy atom sites were found with the anomalous data for the mercury derivative to a resolution of 4.6 Å and the program SOLVE (*16*). The native and derivative data with its anomalous signal and the heavy atom sites were used to build an initial model with the program suite SOLVE/RESOLVE (*17*). The program RESOLVE built 538 residues out of 904 (226 × 4) expected and was able to assign the side chains for 105 of these residues. A model that included 189 out of the 226 possible residues was then constructed by combining the partial models with the 4-fold noncrystallographic symmetry with an iterative RESOLVE/REFMAC5 (*18*) script (http://www.solve.lanl.gov). The R_{work} and R_{free} for this preliminary model were 0.30 and 0.37, respectively. The model was refined with the CNS package (*19*). XtalView (*20*) was used to view the models graphically, to build portions not in the preliminary model, and to adjust the model between refinement cycles. The stereochemistry of the model was checked with PROCHECK (*21*).

Steady State Kinetics. All steady state kinetic experiments were carried out in 50 mM KH_2PO_4 buffer (pH 7.0) at 25 °C as described previously (*22*, *23*). Kinetic parameters of the enzyme with GSH as the variable substrate were determined at a constant concentration of the substrate CDNB (0.2 mM) while the concentration of GSH was varied between 0.2 and 50 mM. Kinetic parameters of the enzyme with CDNB as the variable substrate were determined at a constant, saturating concentration of GSH (100 mM) while the concentration of CDNB was varied between 0.05 and 1.0 mM. Data were fit to the equation for a rectangular hyperbola to obtain k_{cat} and k_{cat}/K_M for each substrate.

Difference Spectroscopy. The pK_a of the thiol of enzyme-bound GSH was determined by UV difference spectroscopy as previously described (*24*). Spectra of the enzyme and the E•GSH complex were recorded on a Perkin-Elmer Lambda 18 spectrophotometer at 25 °C and pH values between 5.0 and 7.8. The difference spectra ([E•GSH] − [E]) were calculated to obtain the intensity of the thiolate absorption band at 240 nm. The buffers used were 0.1 M sodium citrate (pH 5.0 and 5.4) and 0.1 M potassium phosphate (pH 6.0, 6.5, 7.0, 7.5, and 7.8).

Table 2: Final Refinement Statistics for rGSTK1-1

refinement program	CNS
resolution limits (Å)	30.0−2.50
R_{work} (95% of data)	0.204
R_{free} (5% of data)	0.256
hetero groups	glutathione/polypeptide
water molecules	263
bond lengths rms deviation (Å)	0.023
angles rms deviation (°)	1.82
average B (mainchain/side chain/water)	40.4/41.0/38.3

Kinetics of the Binding of Glutathione. Approach to equilibrium kinetic data for glutathione binding were obtained with an Applied Photophysics Ltd. model SX17MV stopped-flow spectrometer at 25 °C with a 0.2 cm path length observation cell. In the absorption mode, the wavelength was set at 240 nm to detect thiolate anion formation. In the fluorescence mode, the excitation was set at 290 nm, and the intrinsic protein fluorescence was observed through a 320 nm cutoff filter. Reactions contained 10 μM enzyme for the absorption measurements and 0.5 μM enzyme for the fluorescence measurements (concentrations observed in the cell). Solutions of enzyme and glutathione were made in 50 mM potassium phosphate buffer (pH 7.0). In general, 5−9 kinetic traces were averaged for each concentration of glutathione and the averaged data fit to a single-exponential equation.

RESULTS

Overall Structure of rGSTK1-1. The structure of rGSTK1-1 was solved with phases derived from a single Hg derivative containing 10 Hg sites in the asymmetric unit. The final refinement statistics for the structure solution are presented in Table 2. The atomic coordinates and structure factors have been deposited with the PDB (PDB file 1R4W). The final model includes residues 2−222 of all four polypeptide chains with no electron density observed for residues 223−226. Two areas in each of the four chains, residues 52−58 and 87−90, have low electron density and high B-factors. Like most canonical GSH transferases, the biological unit of the enzyme is a dimer. However, the domain structure, arrangement, and dimer interfaces of the class kappa enzyme are quite different. Each subunit consists of a thioredoxin-like domain that is interrupted with an all α-helical domain. This is more clearly elicited in Table 3, a summary of the secondary structural elements and the domains with which they are associated. In contrast, all of the canonical GSH transferases have a contiguous thioredoxin-like domain at the N terminus. The difference in domain structures is illustrated in Figure 1.

A probe of the PDB coordinate files with DALI (*25*) indicates that the most closely related known structure is that of dsbA (PDB file 1FVK) from *E. coli*, a protein disulfide bond isomerase. The structural similarity is strong with a *Z*-score of 11.8 over 188 equivalent residues. Importantly, the similarity includes both the interrupted thioredoxin-like domain and the inserted α-helical domain. The most closely related canonical GSH transferase listed in the DALI search is the tau class enzyme, PDB file 1GWC (*6*) with a *Z*-score

Table 3: Arrangement of Secondary Structural Elements in rGSTK1-1

element[a]	residues	domain
β-strand-1	6−12	thioredoxin-like
α-helix-1	16−30	thioredoxin-like
β-strand-2	35−41	thioredoxin-like
α-helix-2	43−51	thioredoxin-like
α-helix-3	59−78	α-helical
α-helix-4	89−95	α-helical
α-helix-5	96−110	α-helical
α-helix-6	113−127	α-helical
α-helix-7	134−145	α-helical
α-helix-8	148−157	α-helical
α-helix-9	161−178	α-helical
β-strand-3	185−190	thioredoxin-like
β-strand-4	193−198	thioredoxin-like
α-helix-10	202−211	thioredoxin-like

[a] The secondary structure was analyzed with PROMOTIF (*27*).

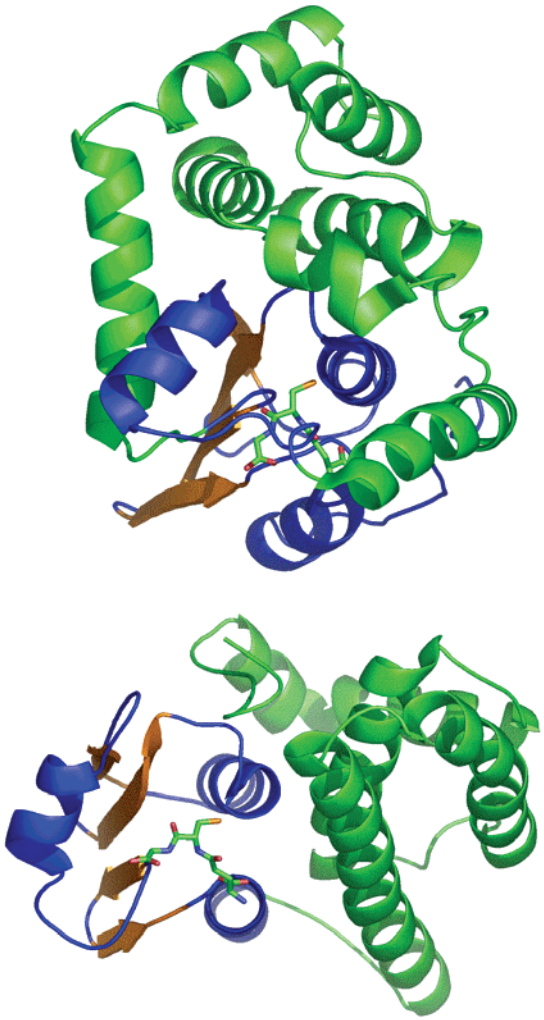

FIGURE 1: Comparison of the domain arrangements of the class kappa polypeptide rGSTK1 (top) with the canonical class mu subunit rGSTM1 (bottom). The thioredoxin-like domains are shown in blue and orange while the nonhomologous α-helical domains are illustrated in green. The GSH molecules are shown in stick representation. The figure was generated with the program PYMOL (*26*).

= 5.7. In this instance, the structural similarity extends only to the thioredoxin-like domains of both proteins.

The interface of the AB dimer of the kappa GSH transferase is extensive and buries 2798 Å^2 of surface area. The structure of the interface is quite different from that observed in the canonical enzymes. The interface positions α-helix-3 of one monomer (residues 59−78) perpendicular to the β-sheet of the opposing subunit with helix-3 packing against α-helix-10 of the opposite subunit with an angle close to 90°. This brings the two GSH binding sites close together as illustrated in Figure 2. The N1 atoms of the bound GSH molecules are 5.4 Å apart. Although many of the interactions at the interface are hydrophobic, there are important electrostatic features as well. For example, the NH_2 group of R202 is within hydrogen-bonding distance of OD2 of E201 while the NE group is within hydrogen-bonding distance of OE2 of E69 of the opposing subunit. As discussed in more detail below, both R202 and E201 constitute an integral part of the GSH binding site.

The kappa dimer has a very different overall shape when compared with the canonical GSH transferase fold (Figure 2). The rGSTK1-1 dimer is quite elongated whereas the canonical dimers are more globular. For example, the tau class enzyme (*6*) (PDB file 1GWC) displays the characteristic V-shaped crevice of the other canonical enzymes when viewed with the 2-fold axis perpendicular to the line of sight, with the N1 atoms of the bound GSH derivatives 15.3 Å apart. In this instance, the main interactions at the dimer interface are between α-helix-3 of the first domain of one monomer and α-helix-4 of the second domain of the other monomer.

Glutathione Binding Site. The two GSH binding sites in the dimer lie near the subunit interface with residues from both subunits participating in the interactions with each GSH molecule. The hydrogen-bonding and electrostatic interactions between the protein and the GSH are less extensive than that observed in many other GSH transferases. For instance, there are no hydrogen-bonding interactions with the γ-glutamyl amide carbonyl or the amide N−H of the glycyl residue. As in the canonical GSH transferases, the γ-glutamyl moiety is recognized by the strand-turn-helix motif located in the second half of the thioredoxin domain as illustrated in Figure 3. The turn harbors S200 with the main chain NH and side chain OH within hydrogen-bonding distance of the carboxylate group of the γ-glutamyl residue and D201, the side chain of which forms an ionic interaction with the γ-glutamylammonium group. Interestingly, the side chain of R202 from the strand-turn-helix motif in the opposite subunit also contributes by providing additional ionic interaction with the carboxylate group of the γ-glutamyl residue.

Electrostatic interactions between the enzyme and the cysteinyl residue of GSH include the hydroxyl group of S16 located at the N-terminal end of α-helix-1, which is within hydrogen-bonding distance of the sulfur and the main chain NH of L183, which is within hydrogen-bonding distance of the carbonyl group of the substrate. The glycyl end of the tripeptide appears to have electrostatic interactions between the carboxylate of the glycine and the side chain NH_2 of N53 and the side chain of K62 from the opposite subunit.

Active Site. The binding site for the electrophilic substrate is less well-defined. The sulfur of GSH lies about 12 Å from the surface of the protein and is accessible by a predominately hydrophobic channel that is roughly 9 Å in diameter as illustrated in Figure 4. The bottom and walls of the channel are composed of residues D13 and L15 between β-strand-1 and α-helix-1; S16, P17, and Y18 from α-helix-1; L44 and

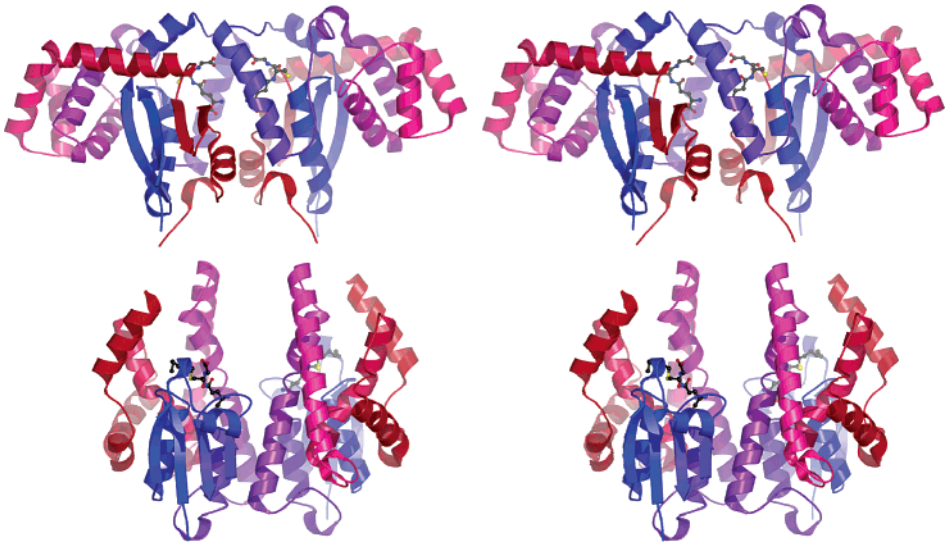

FIGURE 2: Stereo representations of the dimer of rGSTK1-1 in complex with GSH (top) and the tau class GSH transferase in complex with S-hexyl-GSH (PDB file 1GWC) (bottom). The cartoon representations were generated with MOLSCRIPT (*26*, *28*, *29*). Each monomer of the dimer is colored blue at the N terminus and ramps to red at the C terminus. Glutathione and S-hexyl-glutathione molecules are shown in ball-and-stick representation.

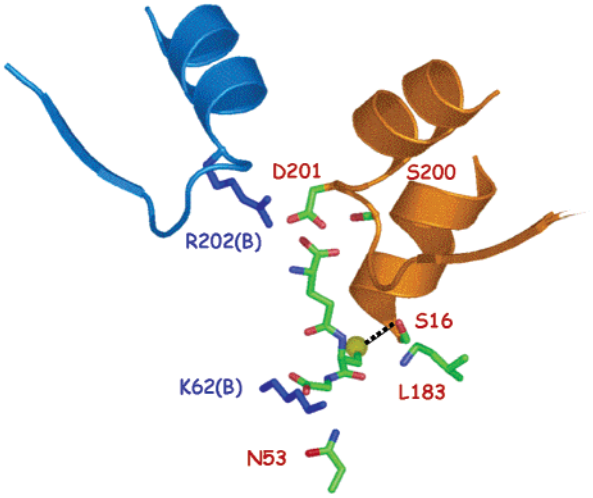

FIGURE 3: Interactions between rGSTK1-1 and GSH. The structural elements in the primary subunit involved in GSH binding are shown in orange with specific residues drawn in stick representation and labeled in red. The GSH molecule is shown in stick representation with the sulfur illustrated as a sphere. The hydrogen-bonding interaction between the sulfur and the hydroxyl group is represented by a dotted line. The structural elements and side chains that participate in GSH binding from the opposite subunit are shown in blue.

A45 in α-helix-2; L67 and I70 from α-helix-3; V92 and K93 from α-helix-4; and W126 from α-helix-6 and L183. The channel is also flanked by two loops, residues 52−58 and 87−90 with poorly defined electron density. The structural model suggests that the side chains of P55, P56, F87, and F88 also contribute to the entrance and walls of the access channel. Interestingly, the disordered surface loops from both subunits contact one another and form a patch that is 15 Å wide and extends diagonally some 50 Å across the protein surface as illustrated in Figure 5.

Interaction of the Enzyme with GSH. The functional interaction of GSH with the enzyme was investigated by UV difference spectroscopy and by stopped-flow kinetics of the approach to equilibrium. The pH dependence of the UV difference spectra ([E•GSH] − [E]) at 240 nm shown in Figure 6 indicates that the pK_a of the thiol of enzyme-bound GSH is 6.4. The extinction coefficient for the thiolate (ϵ_{240} = 5100 M^{-1} cm^{-1}) is in good agreement with results obtained with other GSH transferases (*24*).

Table 4: Rate Constants for Binding of GSH to rGSTK1-1[a]

signal	k_{on} (M^{-1} s^{-1})	k_{off} (s^{-1})	K_d[b] (μM)
A_{240}	(1.25 ± 0.05) × 10^5	4 ± 2	30 ± 20
fluorescence	(0.95 ± 0.02) × 10^5	8.4 ± 1.2	90 ± 10

[a] Uncertainties are standard deviations of the mean value. [b] K_d = k_{on}/k_{off}.

Table 5: Steady State Kinetic Parameters for rGSTK1-1 and the S16A Mutant toward CDNB[a]

enzyme	k_{cat}[b] (s^{-1})	k_{cat}/K_M^{CDNB} [c] (M^{-1} s^{-1})	K_M^{GSH} [b] (mM)
native	280 ± 30	(1.73 ± 0.08) × 10^5	11 ± 1
S16A	8.9 ± 0.2	(1.02 ± 0.06) × 10^4	2.83 ± 0.06

[a] Uncertainties are standard deviations of the mean value. [b] Values of k_{cat} and k_{cat}/K_M^{CDNB} were obtained at saturating [GSH] and CDNB as the variable substrate. [c] Obtained with [CDNB] = 200 μM.

The kinetics of the approach to equilibrium for the binding of GSH to rGSTK1-1 was followed by both fluorescence and absorbance stopped-flow spectroscopy. The time course of the change in intrinsic protein fluorescence on binding GSH is illustrated in Figure 7A. The observed rate constant for the fluorescence change varies as a linear function of [GSH] (Figure 7B) in the concentration range studied (50 μM to 1.6 mM). The apparent rate constants for association and dissociation are summarized in Table 4. The apparent k_{on} is much less than the diffusion limit, and k_{off} is relatively small. The kinetics of thiolate formation followed by UV spectroscopy at 240 nm give very similar results as summarized in Table 4.

Steady State Kinetics and the Function of S16 in Catalysis. The steady state kinetic constants of the rGSTK1-1-catalyzed addition of GSH to CDNB are listed in Table 5. The enzyme exhibits a high turnover number toward CDNB as well as a relatively high K_M^{GSH}. The fact that $K_M^{GSH} \gg K_d^{GSH}$ indicates that the binding of GSH does not come to equilibrium in

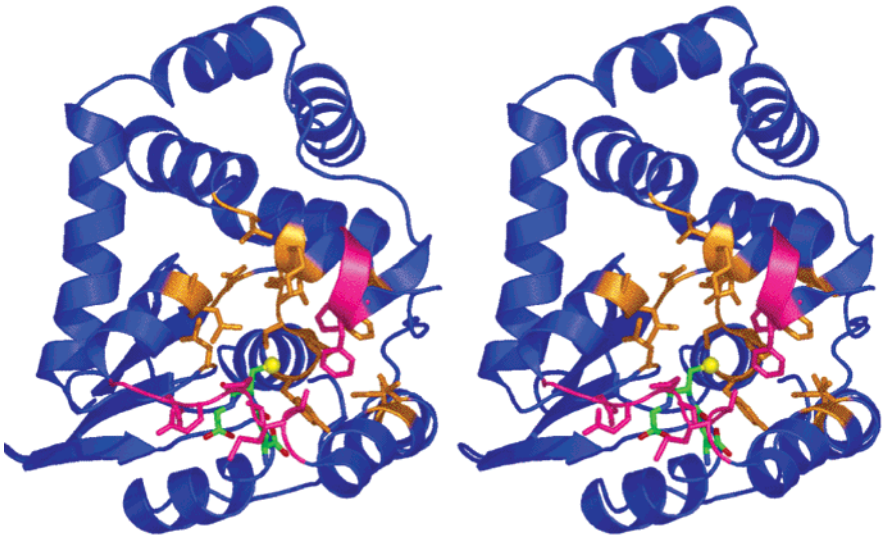

FIGURE 4: Stereoview of the active site access channel. The GSH molecule is shown in stick representation with the sulfur illustrated as a yellow sphere. Residues that contribute to the active site cavity are illustrated in orange stick representation with the two disordered regions colored in magenta.

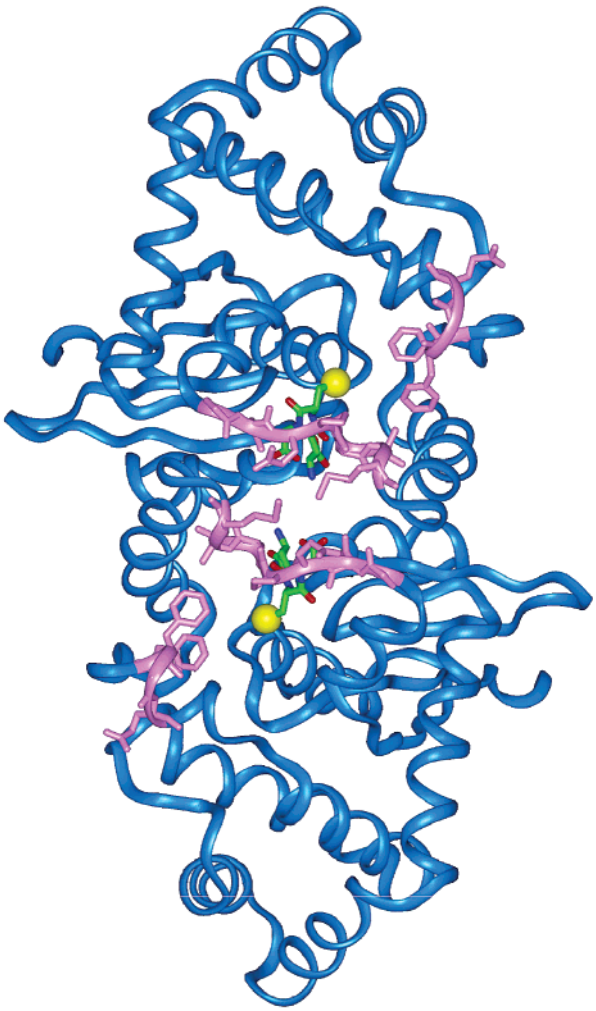

FIGURE 5: View of the loop regions that flank the active site access channels of the AB dimer. The loop regions, residues A52−A58, A87−A90, B52−B58, and B87−B90, which form a large, disordered, and principally hydrophobic patch, are colored pink. The bound GSH molecules at the bottom of the channels are in stick representation with the sulfur shown as yellow spheres.

the steady state reaction with CDNB. The S16A mutant turns over CDNB about 30-fold less efficiently than the native

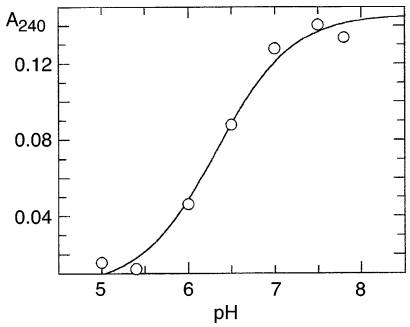

FIGURE 6: Dependence of A_{240} on pH in the UV difference spectrum of [E•GSH] − [E]. The solid line is a fit of the experimental data to a single ionization with a pK_a = 6.4 ± 0.1 and $\Delta\epsilon_{240}$ = 5100 ± 200 M^{-1} cm^{-1}.

enzyme, a result that is consistent with its proximity to the sulfur of GSH in the structure and an important role in catalysis. The mutant has a lower K_M^{GSH}, which again reveals that the value observed with the native enzyme does not accurately reflect the K_d^{GSH}.

DISCUSSION

Functional Attributes of the Interaction of the Enzyme with GSH. The approach-to-equilibrium kinetics for the binding of GSH to rGSTK1-1 indicates that the association of GSH with the enzyme occurs at less than the diffusion limit. This fact and the linear dependence of the k_{obs} on [GSH] are consistent with the binding mechanism illustrated in Scheme 1 and is similar to that previously postulated for the class mu enzyme, rGSTM1-1, where the binding involves a rare conformation of the protein (E*) that is in rapid equilibrium with a less receptive conformational state (*23*). This results in a linear concentration dependence of the observed rate constant for binding of GSH from $k_{obs} = k_{-2} + k_2(k_1/k_{-1})$[GSH] so that the apparent second-order rate constant for the association is $k_2(k_1/k_{-1})$.

The off-rate for the thiolate is slow relative to turnover with a reactive substrate such as CDNB so that binding of GSH and formation of the E•GS^- complex cannot come to equilibrium as illustrated in Scheme 2. This is clearly the

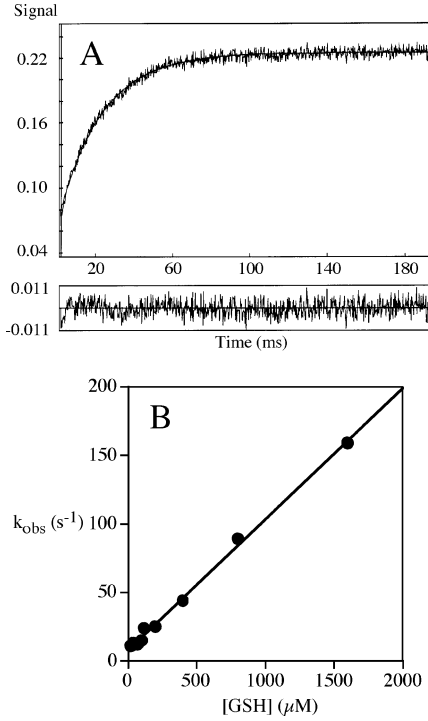

FIGURE 7: (A) Fluorescence change on rapid mixing of rGSTK1-1 and GSH at pH 7.0 and 25 °C. The sample, [E] = 0.5 μM and [GSH] = 400 μM, was excited at 290 nm, and total fluorescence was observed through a 320 nm cutoff filter. The lower trace is the residual to a fit of the data to a single exponential with a k_{obs} = 44.9 ± 0.4 s^{-1}. (B) Dependence of k_{obs} on [GSH]. The line is a least-squares fit of the data to $k_{obs} = k_{off} + k_{on}$[GSH] with a slope = (9.5 ± 0.2) × 10^4 M^{-1} s^{-1} and an intercept = 8.4 ± 1.2 s^{-1}.

Scheme 1

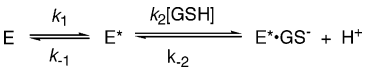

Scheme 2

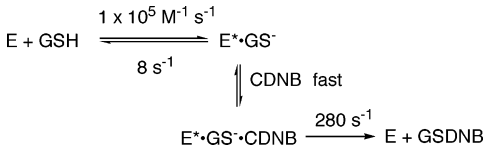

case under the conditions of the steady state assays ([CDNB] = 0.2 mM]) if it is assumed that CDNB binds at or near the diffusion limit (k_{on} > 10^7 M^{-1} s^{-1}). The expected consequence of this on the steady state kinetics is that $K_M^{GSH} \gg K_d^{GSH}$. The ordered binding of the substrates indicated in Scheme 2 is inferred from both the structure, where GSH is bound at the bottom of the active site cavity, and the fact that GSH binds considerably more tightly than CDNB.

Although the k_{cat} of 280 s^{-1} is impressive, it is not known whether this represents the rate of the chemical reaction in the enzyme−substrate complex or the rate of product release. Rate constants for the chemical reaction in the ternary (E•GS^-•CDNB) complex with other GSH transferases are often large, on the order of 500−1200 s^{-1} (*30*, *31*). It is therefore possible that product release is the rate-limiting step in turnover of CDNB by rGSTK1-1.

The three-dimensional structure and the loss of catalytic activity in the S16A mutant suggest that the hydroxyl group of S16 serves to help stabilize the thiolate of bound E•GS^- in much the same way as is proposed for the class theta enzymes (*32*−*35*). It is interesting to note that it was the N-terminal peptide of rGSTK1-1 containing S16 that led to the original proposition that it was related to the theta class enzymes (*8*). The human theta class hGSTT2-2 (PDB file 1LJR) does appear on the output of the DALI search with rGSTK1-1 as the probe structure but with an unimpressive *Z*-score of 2.7 that is limited to the thioredoxin-like domain.

Biological Function of the Mitochondrial GSH Transferases. There are at least two GSH transferases in the mitochondrion, the class kappa enzyme and the membrane-bound enzyme MGST1. The latter enzyme is presumed to be involved in the detoxication of lipid oxidation products (*2*, *36*). At this juncture, the biological role of the class kappa enzyme in the mitochondrion is not known. Considerable amounts of reactive oxygen species are generated during respiration so it has been presumed that rGSTK1-1 has a protective role (*8*−*10*). The structure of the enzyme does not provide any obvious clues in this regard. However, the extensive patch of disordered, hydrophobic loops on the face of the dimer nearest the active site access channels suggests that the protein may dock with a membrane or a protein partner as part of its biological function. At this point, there is no additional biochemical or other physical evidence to support this hypothesis.

Microbial GSH Transferases with the Kappa Fold. It is not generally appreciated that GSH transferases related to the class kappa enzymes are also found in the microbial world and thus widely distributed in biology. The enzyme 2-hydroxychromene-2-carboxylate isomerase, a protein that participates in the catabolism of naphthalene and perhaps other aromatic hydrocarbons in microorganisms (*13*), is closely related to the mammalian class kappa GSH transferase. It exhibits 18% sequence identity over 90% of the polypeptide with rGSTK1-1. A sequence identity of 6−8% would be considered random. More convincingly, five of the seven residues involved in binding GSH are strictly conserved and the remaining two are similar. The level of sequence identity and the conserved binding site suggest that the proteins belong to the same structural superfamily and thus share the same overall fold.

Implications of the Kappa Fold for the Evolution of GSH Transferases. It is clear that the class kappa GSH transferase belongs to a different structural fold than the canonical enzymes. Nevertheless, the functional core of both the canonical and the class kappa enzymes is the thioredoxin-like domain that functions principally as a GSH recognition motif. The remarkable similarity of these domains particularly with respect to the positioning of the GSH molecule (*37*) is illustrated in Figure 8 for glutaredoxin-1(C14S), rGSTK1, and rGSTM1.

Glutaredoxin-1 is a small 85 residue electron transfer protein closely related to thioredoxin with a redox active 11-CPYC-14 motif located at the N-terminal end of the first α-helix. The oxidized form harbors a disulfide bond between C11 and C14 of the 11-CPYC-14 sequence. Reduction of the disulfide is mediated by GSH via a mixed disulfide intermediate between the GSH and the thiol group of C11 (*37*). The equivalent sequence in the thioredoxin-like domain of rGSTK1 is 16-SPYS-19 where the two cysteine residues are replaced by serine. Thus, the hydroxyl group S16 that activates GSH in rGSTK1-1 is positioned similarly to the side chain of C11 that forms the mixed disulfide in

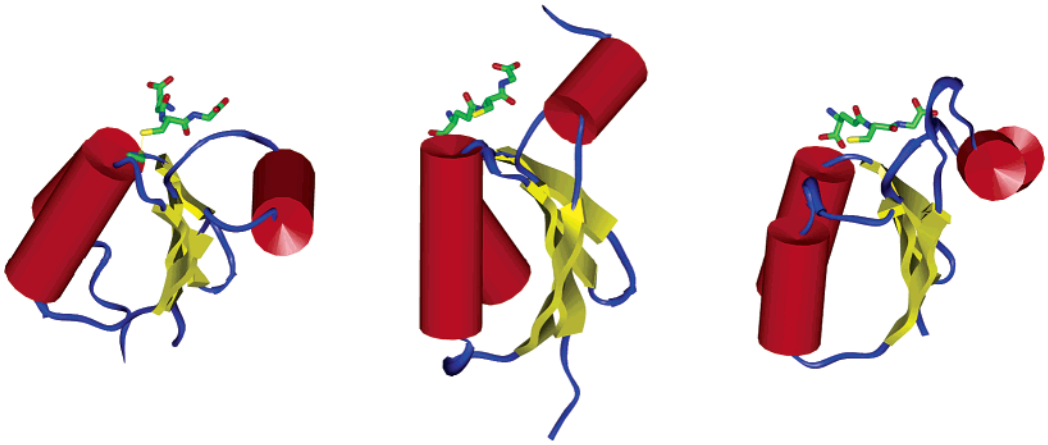

FIGURE 8: Comparison of the thioredoxin domains of glutaredoxin-1(C14S) (left), rGSTK1 (center), and rGSTM1 (right). The glutathione molecules are shown in stick representation.

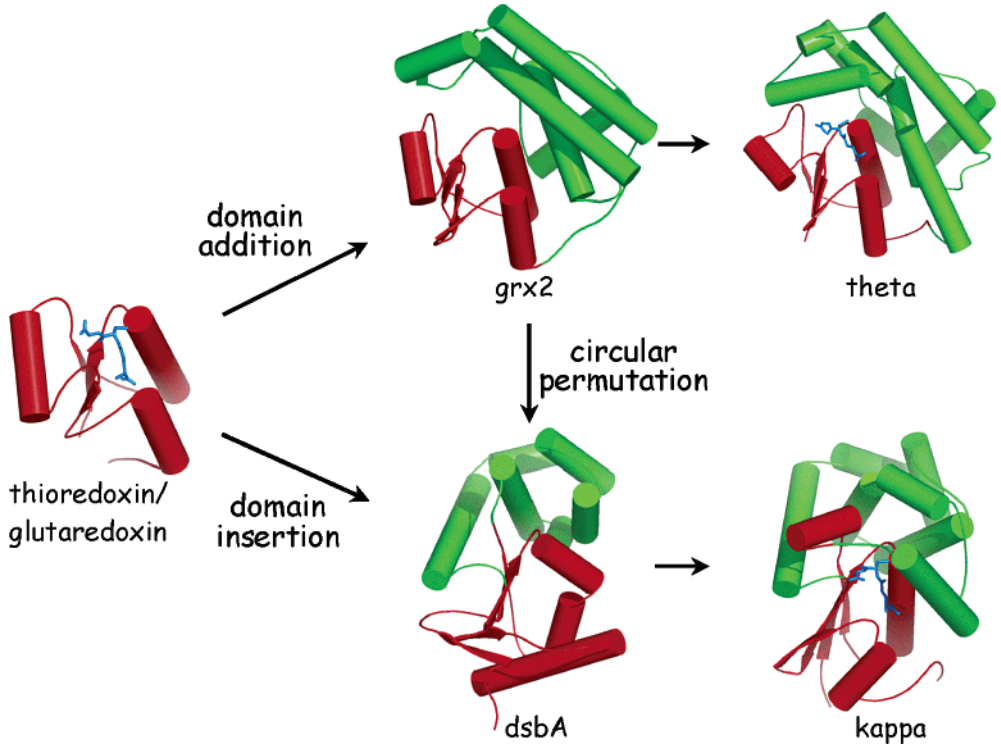

FIGURE 9: Proposed parallel pathways for the evolution of the canonical GSH transferases by domain addition via a grx2-like intermediate (top) and the class kappa GSH transferases by domain insertion or circular permutation of grx2 via a dsbA-like intermediate (bottom). The thioredoxin-like domains are shown in red, the α-helical domains are shown in green, and the glutathione molecules in glutaredoxin-1, the theta and kappa GSH transferases, are shown in blue stick representation.

glutaredoxin-1(C14S). Many of the other noncovalent interactions between the glutathionyl moieties and the three proteins in Figure 8 are conserved even though the domain arrangements and oligomeric states of the proteins are quite different. This is particularly true for the strand-turn-helix motif that essentially acts as a recognition unit for the α-carboxyl- and α-amino groups of the γ-glutamyl moiety.

The electron transfer proteins thioredoxin and glutaredoxin are possible starting points for the evolution of both the canonical and the class kappa GSH transferases, a process that may have occurred by parallel mechanisms as illustrated in Figure 9. Aerobic organisms utilize GSH as an electron donor in a variety of processes including reduction of ribonucleotide reductase and the protection of proteins from oxidation. The former process is mediated by glutaredoxin-1 in *E. coli* while the latter is thought to involve the larger molecule, glutaredoxin-2 (grx2). Both of these proteins share a thioredoxin-like domain where the redox chemistry occurs. However, grx2 has appended to its thioredoxin-like domain an extensive all α-helical C-terminal domain (Figure 9) so that it bears a remarkable resemblance to the canonical GSH transferases (*38*).

From a functional standpoint, it is interesting to consider that as aerobic organisms evolved to utilize GSH as a reductant, they did so by first modifying the thioredoxin scaffold to accommodate the cofactor and eventually to extend the diversity of redox functions. Dyson and coworkers (*38*) suggest that the GSH transferases represent a further functional extension of this fold to the detoxification of electrophiles. Thus, glutaredoxin-1 and grx2 may represent intermediates in the evolution of the canonical GSH transferases from the ancient thioredoxin fold that occurred by a

process of domain addition (Figure 9) to a glutaredoxin progenitor.

What is even more interesting is that the class kappa GSH transferases may have evolved by a parallel pathway involving a domain insertion process and functionally similar intermediates. The protein disulfide bond isomerase, dsbA, is structurally and functionally related to the glutaredoxins but differs structurally by the insertion of an all α-helical domain between α-helix-2 and β-strand-3 of the thioredoxin-like domain. The structure is very similar to the class kappa GSH transferase rGSTK1-1. It seems possible that in two instances proteins involved in glutathione redox chemistry for the protection and proper folding of proteins evolved by distinct but parallel mechanisms to catalyze nucleophilic addition chemistry. Although the pathways for the molecular evolution of the canonical and class kappa enzymes may have initially diverged from a common progenitor, it is likely that the similar mechanistic imperatives for the activation of GSH for thiol-disulfide exchange and nucleophilic addition guided two separate (convergent) structural solutions to the same enzyme activity.

CONCLUSIONS

The class kappa and canonical GSH transferases represent different structural folds that support similar catalytic activity. The GSH binding domains are similar in many respects, a fact that suggests a single progenitor species for this aspect of the enzyme structure and function. The overall fold of the class kappa enzyme and its similarity to dsbA suggest that two distinct superfamilies of GSH transferases have evolved from different thiol-disulfide oxido-reductase progenitors by parallel pathways. This conclusion stands in contrast to the pathway recently proposed by Sheehan et al. (*4*) in which all GSH transferases diverged from a common ancestor. An extensive disordered hydrophobic patch on the dimer surface near the active sites provides the basis for a hypothesis that the enzyme binds to a membrane surface or another protein as part of its function.

REFERENCES

1. Armstrong, R. N. (1997) Catalytic mechanism and evolution of the glutathione transferases, *Chem. Res. Toxicol. 10*, 2−18.
2. Jakobsson, P.-J., Morgenstern, R., Mancini, J., Ford-Hutchinson, A., and Persson, B. (1999) Common structural features of MAPEG-A widespread superfamily of membrane associated proteins with highly divergent functions in eicosanoid and glutathione metabolism, *Protein Sci. 8*, 689−692.
3. Armstrong, R. N. (2000) Mechanistic diversity in a metalloenzyme superfamily, *Biochemistry 39*, 13625−13632.
4. Sheehan, D., Meade, G., Foley, V. M., and Dowd, C. A. (2001) Structure, function and evolution of glutathione transferases: Implications for classification of nonmammalian Members of an ancient enzyme superfamily, *Biochem. J. 360*, 1−16.
5. Board, P. G., Coggan, M., Chelvanayagam, G., Easteal, S., Jermiin, L. S., Schulte, G. K., Danley, D. E., Hoth, L. R., Griffor, M. C., Kamath, A. V., Rosner, M. H., Chrunyk, B. A., Perregaux, D. E., Gabel, C. A., Geoghegan, K. F., and Pandit, J. (2000) Identification, characterization, and crystal structure of the omega class glutathione transferase, *J. Biol. Chem. 275*, 24798−24806.
6. Thom, R., Cummins, I., Dixon, D. P., Edwards, R., Cole, D. J., and Lapthorn, A. J. (2002) Structure of a tau class glutathione S-transferase from wheat active in herbicide detoxification, *Biochemistry 41*, 7008−7020.
7. Kraus, P. (1980) Resolution, purification and some properties of three glutathione transferases from rat liver mitochondria, *Hoppe-Seyler's Z. Physiol. Chem. 361*, 9−15.
8. Harris, J. M., Meyer, D. J., Coles, B., and Ketterer, B. (1991) A novel glutathione transferase (13-13) isolated from the matrix of rat liver mitochondria having structural similarity to class theta enzymes, *Biochem. J. 278*, 137−141.
9. Pemble, S. E., Wardle, A. F., and Taylor, J. B. (1996) Glutathione S-transferase class kappa: Characterization by the cloning of rat mitochondrial GST and identification of a human homologue, *Biochem. J. 319*, 749−754.
10. Jowsey, I. R., Thomson, R. E., Orton, T. C., Elcombe, C. R., and Hayes, J. D. (2003) Biochemical and genetic characterization of a murine class kappa glutathione S-transferase, *Biochem. J. 373*, 559−569.
11. Altschul, S. F., Madden, T. L., Schäffer, A. A., Zhang, J., Zhang, Z., Miller, W., and Lipman, D. J. (1997) Gapped BLAST and PSI-BLAST: a new generation of protein database search programs, *Nucleic Acids Res. 25*, 3389−3402.
12. Martin, J. L., Bardwell, J. C., and Kuriyan, J. (1993) Crystal structure of the DsbA protein required for disulphide bond formation in vivo, *Nature 365*, 464−468.
13. Eaton, R. W. (1994) Organization and evolution of naphthalene catabolic pathways: sequence of the DNA encoding 2-hydroxychromene-2-carboxylate isomerase and trans-o-hydroxybenzylidenepyruvate hydratase-aldolase from the NAH7 plasmid, *J. Bacteriol. 176*, 7757−7762.
14. Pflugrath, J. W. (1999) The finer things in X-ray diffraction data collection, *Acta Crystallogr. D55*, 1718−1725.
15. Otwinowski, Z., and Minor, W. (1996) Processing of X-ray diffraction data collected in oscillation mode, *Methods Enzymol. 277*, 307−326.
16. Terwilliger, T. C., and Berendzen, J. (1999) Automated MAD and MIR structure solution, *Acta Crystallogr. D55*, 849−861.
17. Terwilliger, T. C. (2002) Automated structure solution, density modification and model building, *Acta Crystallogr. D58*, 1937−1940.
18. Murshudov, G. N., Vagin, A. A., and Dodson, E. J. (1997) Refinement of Macromolecular Structures by the Maximum-Likelihood Method, *Acta Crystallogr. D53*, 240−255.
19. Brünger, A. T., Adams, P. D., Clore, G. M., DeLano, W. L., Gros, P., Grosse-Kunstleve, Jiang, J.-S., Kuszewski, J., Nilges, M., Pannu, N. S., Read, R. J., Rice, L. M., Simonson, T., and Warren, G. L. (1998) Crystallography & NMR system: A new software suite for macromolecular structure determination, *Acta Crystallogr. D54*, 905−921.
20. McRee, D. E. (1999) *Practical Protein Crystallography*, 2nd ed., Academic Press, San Diego.
21. Laskowski, R. A., MacArthur. M. W., Moss, D. S., and Thornton, J. M. (1993) *PROCHECK*: a program to check the stereochemical quality of protein structures, *J. Appl. Crystallogr. 26*, 283−291.
22. Liu, S., Zhang, P., Ji, X., Johnson, W. W., Gilliland, G. L., and Armstrong, R. N. (1992) Contribution of tyrosine 6 to the catalytic mechanism of isoenzyme 3-3 of glutathione S-transferase, *J. Biol. Chem. 267*, 4296−4299.
23. Parsons, J. F., Xiao, G., Gilliland, G. L., and Armstrong, R. N. (1998) Enzymes Harboring Unnatural Amino Acids. Mechanistic and structural analysis of the enhanced catalytic activity of a glutathione transferase containing 5-fluorotryptophan, *Biochemistry 37*, 6286−6294.
24. Graminski, G. F., Kubo, Y., and Armstrong, R. N. (1989) Spectroscopic and kinetic evidence for the thiolate anion of glutathione at the active site of glutathione S-transferase, *Biochemistry 28*, 3562−3568.
25. Holm, L., and Sander, C. (1993) Protein structure comparison by alignment of distance matrixes, *J. Mol. Biol. 233*, 123−138.
26. DeLano, W. L. PYMOL (The PyMOL Molecular Graphics System [http://www.pymol.org]).
27. Hutchinson, E. G., and Thornton, J. M. (1996) PROMOTIF- -a program to identify and analyze structural motifs in proteins, *Protein Sci. 5*, 212−220.
28. Bacon, D. J., and Anderson, W. F. (1988) A fast algorithm for rendering space-filling molecule pictures, *J. Mol. Graphics 6*, 219−220.
29. Merritt, E. A., and Bacon, D. J. (1997) Raster3D: Photorealistic molecular graphics, *Methods Enzymol. 277*, 505−524.
30. Morgenstern, R., Svensson, R., Bernat, B. A., and Armstrong, R. N. (2001) Kinetic Analysis of the Slow Ionization of Glutathione by Microsomal Glutathione Transferase MGST1, *Biochemistry 40*, 3378−3384.
31. Codreanu, S. G., Ladner, J. E., Xiao, G., Stourman, N. V., Hachey, D. L., Gilliland, G. L., and Armstrong, R. N. (2002) Local protein

dynamics and catalysis: Detection of segmental motion associated with rate-limiting product release by a glutathione transferase, *Biochemistry 41*, 15161−15172.
32. Wilce, M. C. J., Board, P. G., Feil, S. C., and Parker, M. W (1995) Crystal structure of a theta-class glutathione transferase, *EMBO J. 14*, 2133−2143.
33. Rossjohn, J., McKinstry, W. J., Oakley, A. J., Verger, D., Flanagan, J., Chelvanayagam, G., Tan, K.-L., Board, P. G., and Parker, M. W. (1998) Human Theta class glutathione transferase: The crystal structure reveals a sulfate-binding pocket within a buried active site. *Structure 6*, 309−322.
34. Board, P. G., Coggan, M., Wilce, M. C. J., and Parker, M. W. (1995) Evidence for an essential serine residue in the active site of the theta class glutathione transferases, *Biochem. J. 311*, 247−250.
35. Jemth, P., and Mannervik, B. (2000) Active site serine promotes stabilization of the reactive glutathione thiolate in rat glutathione transferase T2-2. Evidence against proposed sulfatase activity of the corresponding human enzyme, *J. Biol. Chem. 275*, 8618−8624.
36. Mosialou, E., Piemonte, F., Anderson, C., Vos, R. M. E., van Bladeren, P. J., and Morgenstern, R. (1995) *Arch. Biochem. Biophys. 320*, 210−216.
37. Bushweller, J. H., Billeter, M., Holmgren, A., and Wuthrich, K. (1994) The Nuclear Magnetic Resonance Solution Structure of the Mixed Disulfide between *Escherichia coli* Glutaredoxin(C14S) and Glutathione, *J. Mol. Biol. 235*, 1585−1597.
38. Xia, B., Vlamis-Gardikas, A., Holmgren, A., Wright, P. E., and Dyson, H. J. (2001) Solution structure of *Escherichia coli* glutaredoxin-2 shows similarity to mammalian glutathione-S-transferases, *J. Mol. Biol. 310*, 907−918.

BI035832Z